Evaluation of DNA/Ligand Interactions by Electrospray Ionization Mass Spectrometry

Jennifer S. Brodbelt

Department of Chemistry and Biochemistry, University of Texas, Austin, Texas 78712; email: jbrodbelt@mail.utexas.edu

Annu. Rev. Anal. Chem. 2010. 3:67–87

First published online as a Review in Advance on February 5, 2010

The *Annual Review of Analytical Chemistry* is online at anchem.annualreviews.org

This article's doi: 10.1146/annurev.anchem.111808.073627

1936-1327/10/0719-0067$20.00

Key Words

tandem mass spectrometry, noncovalent complexes, DNA/drug complex, binding affinity, binding selectivity

Abstract

Electrospray ionization mass spectrometry (ESI-MS) has enabled the detection and characterization of DNA/ligand complexes, including evaluation of both relative binding affinities and selectivities of DNA-interactive ligands. The noncovalent complexes that are transferred from the solution to the gas phase retain the signature of the native species, thus allowing the use of MS to screen DNA/ligand complexes, reveal the stoichiometries of the complexes, and provide insight into the nature of the interactions. Ligands that bind to DNA via metal-mediated modes and those that bind to unusual DNA structures, such as quadruplexes, are amenable to ESI. Chemical probe methods applied to DNA/ligand complexes with ESI-MS detection afford information about ligand-binding sites and conformational changes of DNA that occur upon ligand binding.

1. INTRODUCTION

The therapeutic functions of many anticancer and antibacterial drugs stem from their noncovalent interaction with DNA substrates, including DNA duplexes and DNA quadruplexes (1–6). The growing interest in the development and characterization of DNA-interactive agents has amplified the need for sensitive and versatile analytical techniques that are capable of characterizing the binding modes, sequence selectivities, and binding affinities of these compounds, as well as the structures of the resulting DNA/ligand complexes (7–9). Electrospray ionization mass spectrometry (ESI-MS) has emerged as a versatile tool for the analysis of noncovalent DNA/ligand complexes due to its excellent sensitivity, high-throughput screening capabilities, and minimal sample consumption. ESI allows noncovalent complexes to be transferred to the gas phase for subsequent analysis by MS, and auxiliary methods, such as tandem MS (MS/MS) and ion mobility, allow more detailed characterization of the structures of the complexes. Determination of molecular mass reveals the stoichiometries of DNA/ligand complexes, and measurement of ion abundances for different combinations of DNA and ligands gives insight into relative binding affinities and sequence selectivities. The development of ESI-MS as an analytical tool for the analysis of noncovalent DNA/ligand complexes is the focus of this review.

The design, synthesis, isolation, and evaluation of ligands that bind to DNA are active areas in medicinal chemistry and pharmaceutical research (1–6). These types of ligands are currently used to treat a broad array of diseases ranging from malaria and human immunodeficiency virus to a variety of bacterial infections and cancers. Many of these ligands share a common mode of action that involves causing conformational changes or damage to the DNA targets, thus interfering with DNA transcription or prohibiting replication and ultimately interrupting cell growth and proliferation. Often the formation of noncovalent complexes with DNA serves as a prelude to DNA cleavage or inhibition of DNA-associated enzymes. Despite the recognition of the clinical importance of DNA interactive ligands, there continue to be significant gaps in our knowledge about their mechanisms of action, in addition to substantial interest in developing more selective ligands to reduce side effects upon chemotherapeutic use.

Some of the best-known DNA-interactive ligands are those that bind to duplex DNA, via either intercalation or minor groove binding (1–6). The latter ligands are often crescent shaped and thus are well adapted to interact with the curved minor groove of DNA via van der Waals, hydrogen bonds, and hydrophobic interactions. Examples include Hoechst 33342, netropsin, and distamycin (**Figure 1**). These compounds display common selectivity for A/T-rich sequences due to hydrogen-bonding interactions between the ligands and adenines and thymines, interactions that are enhanced by the narrower width of the minor groove of the A/T tracts. There is little evidence to suggest that DNA undergoes substantial conformational changes upon interacting with these ligands, but binding of transcription factors to DNA can be disrupted.

Intercalators often contain one or more planar, aromatic groups that may insert between adjacent base pairs in DNA duplexes. This type of interaction causes separation of the base pairs, partial unwinding near the site of intercalation, and overall elongation of the DNA. Intercalation preferentially occurs at G/C-rich sequences (CpG sites) because these sequences are more easily unstacked. Intercalators generally cause more significant distortion of the native conformations of DNA, a factor that contributes to their disruption of protein binding. **Figure 1** shows the structures of daunomycin and actinomycin D, both common intercalating compounds. Echinomycin is a bis-intercalator, containing two quinoxaline intercalating groups, that leads to a higher binding constant.

Another type of DNA-interactive ligand includes those that bind to quadruplex DNA, a higher-order structure consisting of stacked G-tetrads stabilized by monovalent cations coordinated

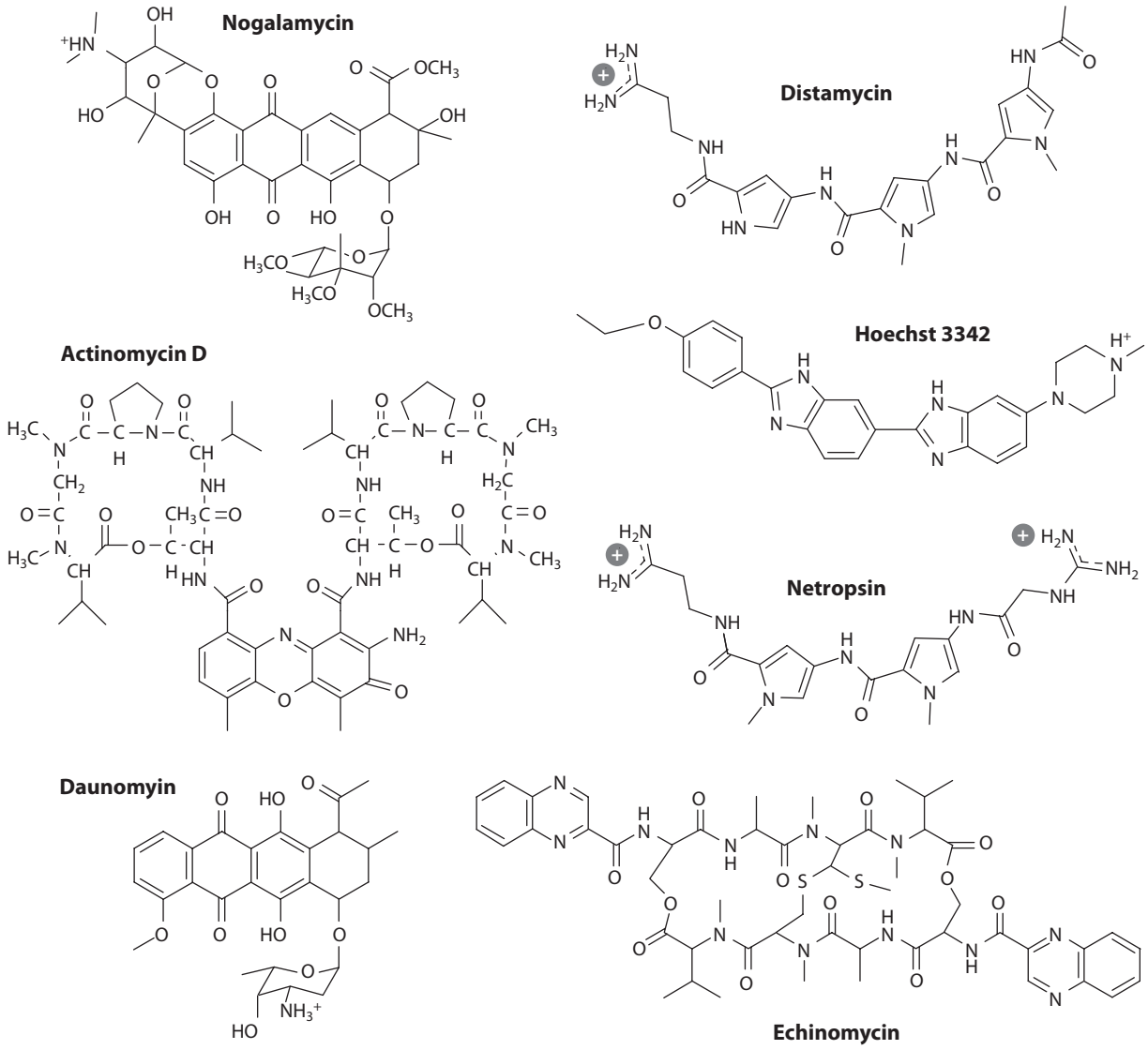

Figure 1

Structures of some common DNA-interactive agents.

to the central cavity (4). Perhaps the most significant quadruplexes evolve from 3′ overhangs of the human telomeric sequence, 5-TTAGGG-3′. Telomeres, which are located on the termini of chromosomes, protect DNA from degradation and signal cell death according to the length of the telomere, which shortens upon DNA replication. Telomerase, a reverse transcriptase enzyme overexpressed in most tumor cells, maintains the length of the telomeres and is thus associated with one of the hallmarks of malignant tumors, cell immortality. Ligands that stabilize quadruplex DNA, either by intercalation or by end stacking, can inhibit telomerase; they thus represent another approach for fighting cancer. Ethidium bromide, an intercalator, and perylene diimides, end-stacking compounds, are examples of ligands that interact with quadruplex DNA.

2. ELECTROSPRAY IONIZATION TO TRANSFER DNA/LIGAND COMPLEXES INTO THE GAS PHASE

The development of ESI in the late 1980s (10) revolutionized the analysis of biological molecules and noncovalent complexes by MS. ESI is a gentle ionization method that allows noncovalent complexes to be transferred from the solution to the gas phase while preserving many of the native interactions. It also results in the production of multicharged ions, which means that even complexes with large molecular weights can be detected with *m/z* values that can be routinely measured by inexpensive mass analyzers such as quadrupoles and quadrupole ion traps. ESI is compatible with both aqueous and nonaqueous solutions, including those that contain low levels of metal salts, and can be used to generate both positive and negative ions. These attributes make ESI a natural choice for the analysis of DNA and DNA/ligand complexes by MS (7–9). The analysis of DNA duplexes through use of ESI-MS was first demonstrated by Smith et al. (11) in 1993; reports of the analysis of DNA/drug complexes followed in 1994 (12, 13). An example of ESI mass spectra for DNA duplex/ligand complexes is shown in **Figure 2** for solutions consisting of the duplex d(GGGACACTGAGGGG/CCCCTCACTGTCCC) with one of two bis-intercalator ligands whose structures differ only in the peptide linker: One has a polyglysine linker (BI-1), and the other has a slightly elongated polyalanine backbone (BI-2). The ESI mass spectra display some ligand-free duplex ions as well as 1:1 and 1:2 duplex/ligand complexes. These particular products are observed in the 5− or 6− charge states. The abundances of the duplex/ligand complexes relative to the ligand-free duplexes are very different in **Figure 2*a*** and ***b***, with far more abundant duplex/ligand complexes observed for BI-1 in **Figure 2*a***. Comparison of the spectra in **Figure 2** reveals that ligand BI-1 demonstrates a higher duplex-binding affinity. It is this type of comparison

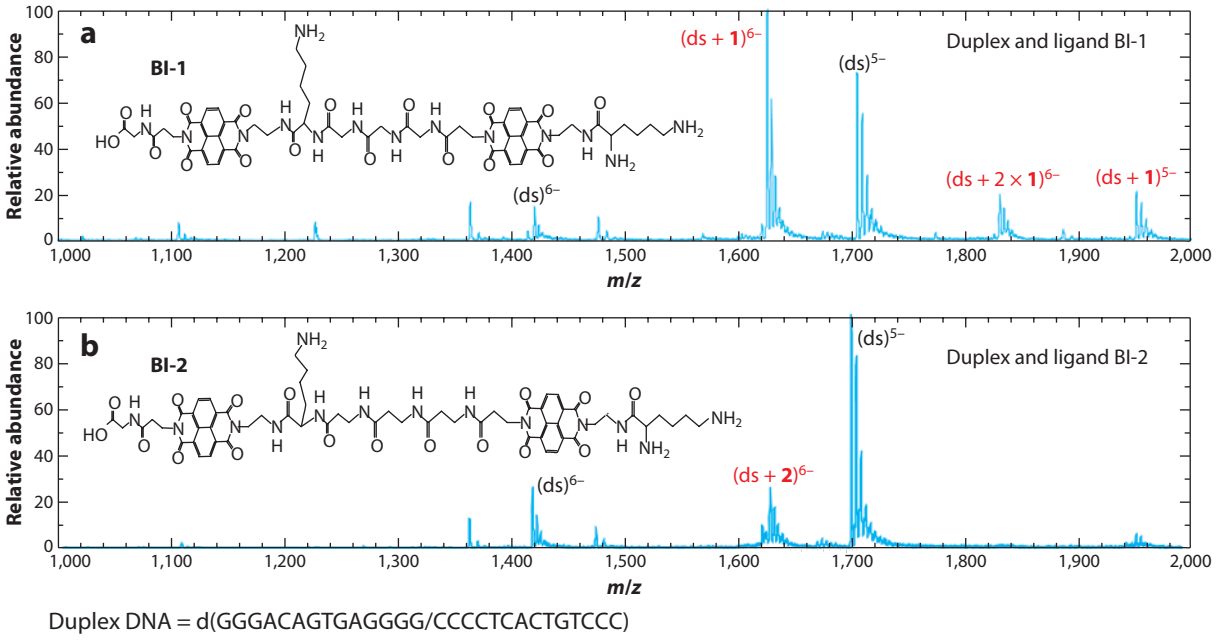

Figure 2

Electrospray ionization mass spectra for solutions containing 10 μM duplex d(GGGACAGTGAGGGG/CCCCTCACTGTCCC) (ds) incubated with (*a*) 10 μM ligand polyglysine linker (BI-1) or (*b*) 10 μM ligand polyalanine backbone (BI-2) in 50 mM NH_4OAc and 25% methanol.

that allows facile assessment of the relative binding affinities of DNA-interactive ligands. Sequence selectivities can likewise be evaluated by ESI-MS, in which case DNA-interactive ligands are incubated with different duplexes and the resulting abundances of the duplex/ligand complexes are used to estimate the relative affinities for the different DNA sequences.

2.1. Electrospray Ionization Mass Spectrometry Analysis of Duplex DNA/Drug Complexes

Early studies of drug/DNA complexes by ESI-MS focused on examining the binding of commercially available drugs to duplex DNA to determine whether the binding behavior observed by MS mirrored known solution activity. In seminal studies by Gale & Smith (12) and Gale et al. (13), the authors examined complexes formed between minor groove binders, including distamycin, pentamidine, and Hoechst 33258 and a self-complementary 12-mer duplex. The binding stoichiometries of the DNA complexes containing the minor groove binders observed in the mass spectra were consistent with previous nuclear magnetic resonance reports. This study also established optimal experimental conditions for the analysis of drug/DNA complexes by ESI-MS, including the use of low ESI voltages and heated capillary temperatures, as well as the use of an ammonium acetate buffer instead of conventional alkali metal buffers. Ammonium acetate is very amenable to ESI-MS because of the greater lability of the ammonium ion over Na^+ and K^+, which reduces the extent of counterion adduction to the DNA ions, in turn leading to less cluttered spectra and better sensitivity.

The first phase of ESI-MS investigations was a systematic one that examined the types of complexes formed between small DNA duplexes and DNA-interactive ligands under a variety of solution and ESI conditions (14–20). These ESI-MS studies collectively showed that MS could be used to assess the sequence selectivity of ligands as well as the stoichiometries of the complexes. The relative binding affinities of the ligands for specific duplexes were evaluated on the basis of competitive binding experiments that involved ESI-MS analysis of solutions containing one duplex with two ligands.

On the basis of the promising correlations obtained between the mass spectrometric results and the known binding properties of the ligands in solution, the De Pauw group (21, 22) pursued the use of ESI-MS data to derive equilibrium association constants for duplex/ligand complexes. The authors calculated the equilibrium association constants by dividing the abundance of the complex of interest (such as a 1:1 duplex/ligand complex) by the product of the abundances of the free duplex and the free ligand in the ESI mass spectra. This simple equation evolved from the assumption that the ESI efficiencies were comparable for the free duplexes and the duplex/ligand complexes. Good agreement was obtained with the equilibrium association constants obtained by standard solution methods, such as fluorescence titrimetry, for complexes containing 12–base pair duplexes. This method was further refined by incorporation of a correction factor, which compensated for differences in ESI efficiencies (known as response factors) (22). The agreement in association constants was admirable given the simplicity of the ESI-MS method, especially in light of the notoriously large standard deviations typically reported for association constants measured by conventional means (3).

These early ESI-MS studies of noncovalent complexes of duplex DNA with commercially available compounds demonstrated a strong correlation between the mass spectrometric results and known solution behavior; they also established a solid foundation for using ESI to transfer complexes from the solution to the gas phase so as to maintain the DNA-interactive properties of the ligands. The challenge of evaluating and understanding the nature of DNA/ligand interactions increases when less well characterized DNA-interactive ligands—those that have metal-mediated

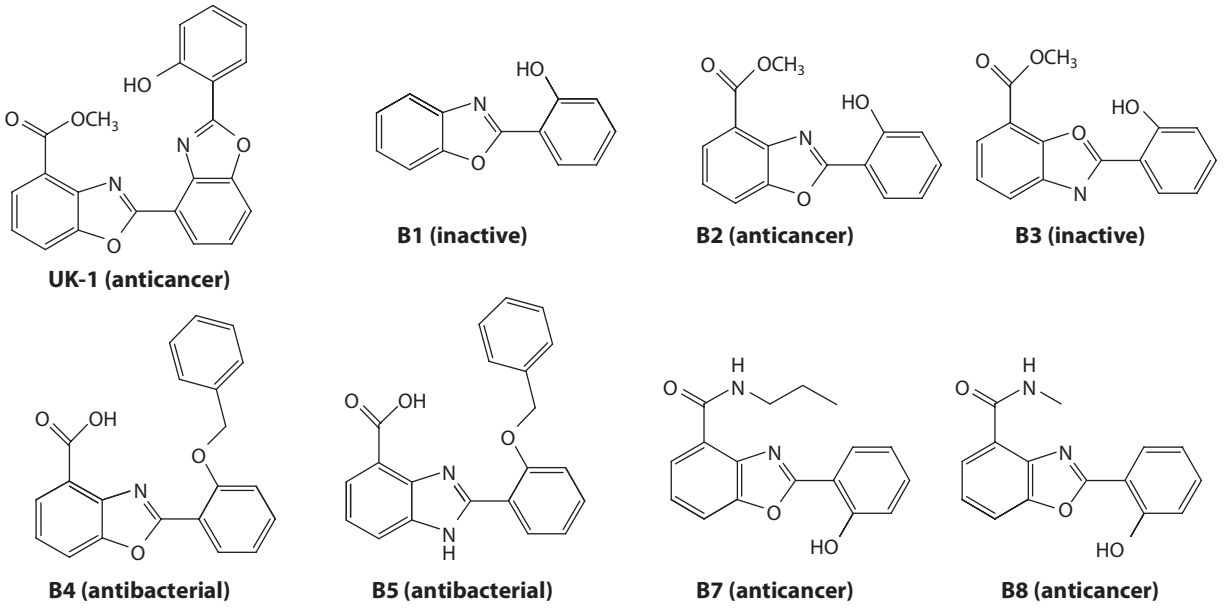

Figure 3

Structures of benzoxazole and benzimidazole compounds.

binding modes or those that exhibit mixed binding modes—are involved. ESI-MS has proven to be useful for exploring DNA/ligand complexation in this context (23–25). One of the original studies reported the use of ESI-MS to examine the metal-mediated binding of chromomycin A_3 and mithramycin, two antitumor agents (23). The authors showed that both chromomycin and mithramycin interacted preferentially with G/C-rich duplexes with ligand:metal stoichiometries of 2:1. Comparing the ion abundances obtained upon ESI of solutions containing different duplexes, different ligands, and different metals led to the determination that the G/C-rich duplexes displayed a higher affinity for chromomycin than for mithramycin. Moreover, subtle differences in the influence of the metal ion were revealed by ESI-MS analysis of solutions containing one duplex, either mithramycin or chromomycin, and one of an array of metal salts. For example, duplex/ligand/metal complexes that incorporated Ni^{2+} or Co^{2+} were readily formed, but complexes containing another transition metal, Zn^{2+}, were formed only in low abundance for duplex/mithramycin complexes.

The metal-mediated binding of a series of benzoxazole and benzimidazole ligands (**Figure 3**) has also been investigated. In these studies (24, 25), solutions containing DNA, one ligand, and either one divalent metal or no metal were analyzed by ESI-MS. These ligands were developed as analogs of UK-1, a natural product isolated from *Streptomyces* that possesses strong anticancer activity presumed to arise from its metal-mediated catalytic inhibition of human topoisomerase II. The binding of divalent metal ions by these ligands affords cationic complexes with increased electrostatic attraction toward DNA and may involve shared coordination of the ligand and phosphate groups on the DNA with the metal ion. The analogs were designed both to provide simpler compounds that may retain potent anticancer activity as well as to allow more detailed examination of the structural basis for the anticancer properties. Examples of ESI mass spectra that illustrate the metal-mediated properties of the ligands are shown in **Figure 4**. The anticancer activity of

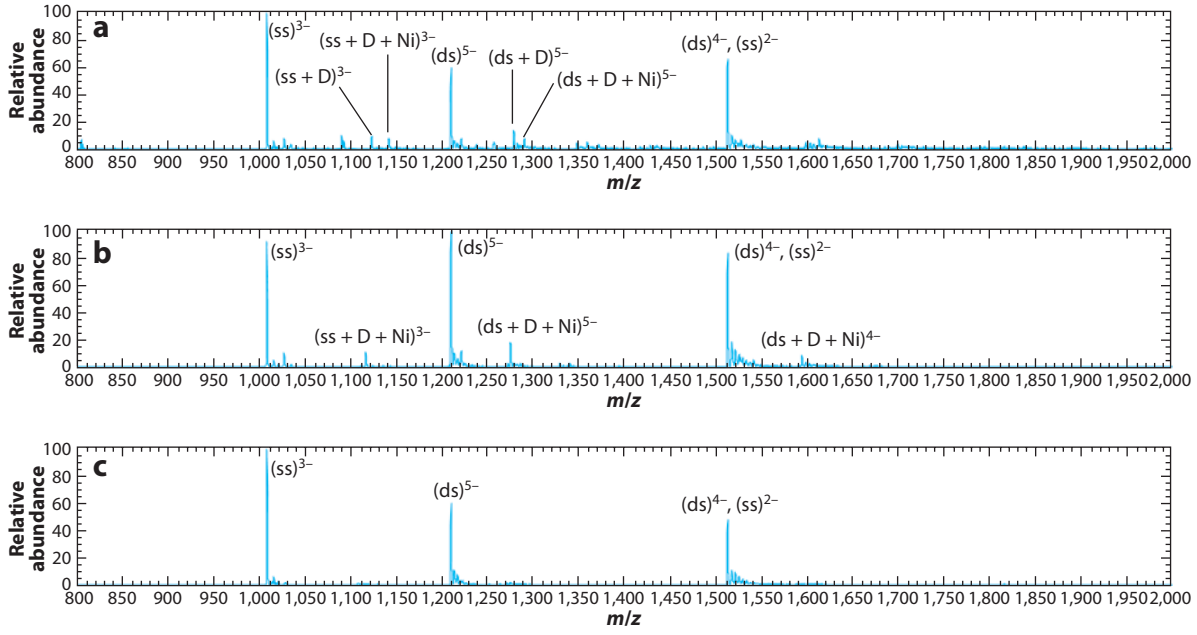

Figure 4

Electrospray ionization mass spectra of solutions containing 5′-GCGAATTCGC-3′ and Ni^{2+} with (*a*) B**4**, (*b*) B**2**, and (*c*) B**1**. Ligand B**2** exhibits the most significant selective metal-mediated binding to the duplex and that B**1** shows no interaction with the duplex. On the basis of the ESI mass spectra, it was determined that two of the benzoxazole compounds (B**4** and B**5**) demonstrated nonspecific DNA binding that was not metal mediated. These compounds exhibited antibacterial but not anticancer activities, as determined by cell assays. Two ligands (B**1** and B**3**) proved to be inactive and displayed no DNA binding, and the final compound (B**2**), which showed anticancer activity, demonstrated metal-mediated binding to DNA with a selectivity for Ni^{2+} over Mg^{2+} or Zn^{2+}. Abbreviations: D, ligand; ds, ligand-free duplex ion. Reprinted with permission from Reference 24. Copyright 2004, Elsevier.

the compounds shown in **Figure 4**, but not their antibacterial activity, correlated with whether the ligand bound to DNA in a metal- or nonmetal-mediated manner.

A subsequent ESI-MS study of benzoxazole ligands possessing different amide- and ester-linked side chains revealed that extension of the side chains resulted in a loss of both the metal-mediated binding behavior and the cytotoxicities (24). For the complexes containing short side chains, 2:1 ligand:metal ion–binding stoichiometries were predominant, whereas the compounds with longer glycol side chains formed abundant 1:1 complexes. Two ligands that exhibited the greatest cytotoxicity against the A549 lung cancer cell line were B**7** (41 μM) and B**8** (14 μM); the latter had an IC_{50} (half maximal inhibitory concentration) value similar to that of B**2** (12 μM). In particular, B**7** and B**8** displayed the most significant degree of metal-mediated DNA binding, as their fraction of bound DNA values increased from zero in the absence of metal ions to 0.40 and 0.27, respectively, in the presence of Cu^{2+}. Of the ligands that exhibited only metal-mediated DNA-binding behavior, the complexation of B**7** and B**8** was enhanced most dramatically by Cu^{2+}. This second study confirmed that the ligands that showed the most significant metal-mediated DNA binding were the ligands that also displayed the greatest cytotoxicities against the A549 lung cancer and MCF7 breast cancer cell lines (24).

ESI-MS has also been used to evaluate the DNA-binding properties of novel ligands designed to increase DNA-binding selectivity or antitumor activity (26). For example, the DNA-binding properties of a series of bis-intercalators containing two naphthalene diimide units connected

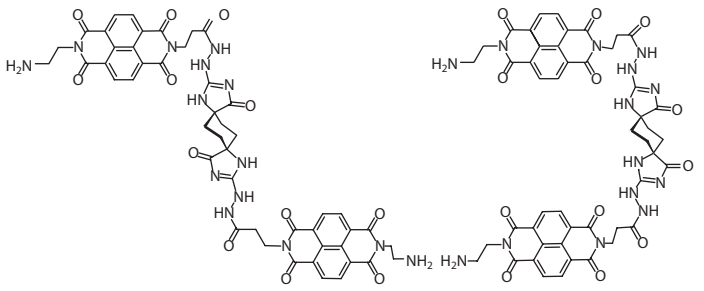

Duplex	*cis*-**C1**	*trans*-**D1**
d(GGGCGGTACCGCGG/ CCGCGGTACCGCCC)	0.86	0.40
d(GCGGGGATGGGGCG/ CGCCCCATCCCCGC)	0.52	0.94
d(GCGGGAATTGGGCG/ CGCCCAATTCCCGC)	0.39	0.64
d(GCGGAAATTTGGCG/ CGCCAAATTTCCGC)	0.32	0.18
d(GGGGTCGCCGGGGG/ CCCCCGGCGACCCC)	0.38	0.78

Figure 5

Structures of two bis-intercalator ligands and their fraction-bound values for interaction with a series of DNA duplexes. Reprinted with permission from Reference 26. Copyright 2007, Elsevier.

by a modifiable scaffold were investigated by parallel ESI-MS and DNAse footprinting methods (26). These compounds are termed threading polyintercalators because one of the functional groups attached to the diimide nitrogen resides in the DNA major groove, whereas the other is in the minor groove upon intercalation of the ligand. Two bis-intercalators, *trans*-**D1** and *cis*-**C1,** possessed a more rigid spiro-tricyclic scaffold (**Figure 5**). ESI mass spectra of solutions containing these ligands and duplexes containing 14 base pairs resulted in detection of complexes with 1:1 or 1:2 DNA:ligand-binding stoichiometries.

A series of duplexes with varying amounts of G/C– and A/T–base pair content was used to evaluate G/C– versus A/T–base pair selectivity of the two isomeric ligands. As the A/T content increased, both the binding stoichiometry and relative abundance of the complexes formed between *trans*-**D1** and the duplex decreased. *trans*-**D1** formed the most abundant complexes with the most G/C-rich duplex, with ligand/DNA binding stoichiometries of 2:1 and 1:1 and little unbound DNA in the spectrum. Although both ligands exhibited G/C–base pair selectivity, the preference was more pronounced for *trans*-**D1** than for *cis*-**C1**. The overall extent of complexation was calculated by expressing the sum of the abundances of ions from DNA/ligand complexes as a fraction of the total abundances of all ions from DNA. The so-called fraction-bound values provide a convenient way to estimate relative binding affinities of DNA-interactive compounds based on the following equation:

$$\text{Fraction of bound DNA} = \frac{A_{(1:1)} + A_{(1:2)} + A_{(1:3)} + \ldots}{A_{(\text{DNA})} + A_{(1:1)} + A_{(1:2)} + A_{(1:3)} + \ldots},$$

where $A_{(\text{DNA})}$ is the peak area of the free duplex species and $A_{(1:n)}$ are the peak areas of all DNA/ligand complexes in the ESI mass spectra. The peak areas of the free and bound DNA ions are assumed to be proportional to their relative concentrations in solution. Greater fraction-bound values signify greater binding affinities. The results summarized in **Figure 5** are consistent with solution dissociation kinetics experiments in which *cis*-**C1** and *trans*-**D1** demonstrated a strong preference for binding to poly(dGdC) over poly(dAdT) sequences. The observed poly(dGdC) preference of the ligands was thought to stem from (*a*) enhanced hydrogen bonding between the intercalators and functional groups in the major and minor grooves of G/C-rich sequences as well as (*b*) more favorable electrostatic interactions between the imide carbonyls of the naphthalene diimide groups and the N^2 amino group on G/C base pairs. The sequence selectivities of *cis*-**C1**

Ligand	R1	R2	R3	R4
AP1	H	Cl	CH_3	OH
AP2	H	Cl	CH_3	Cl
AP3	H	Cl	H	OH
AP4	H	Cl	H	Cl
AP7	Cl	H	H	OH
AP9	Cl	H	CH_3	OH
AP10	H	N*	H	OH
AP11	H	N*	CH_3	OH
AP14	N*	H	CH_3	OH

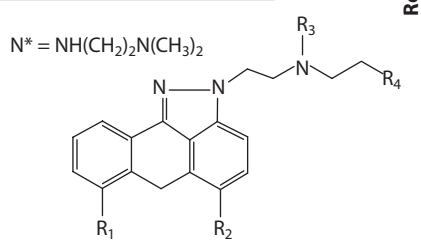

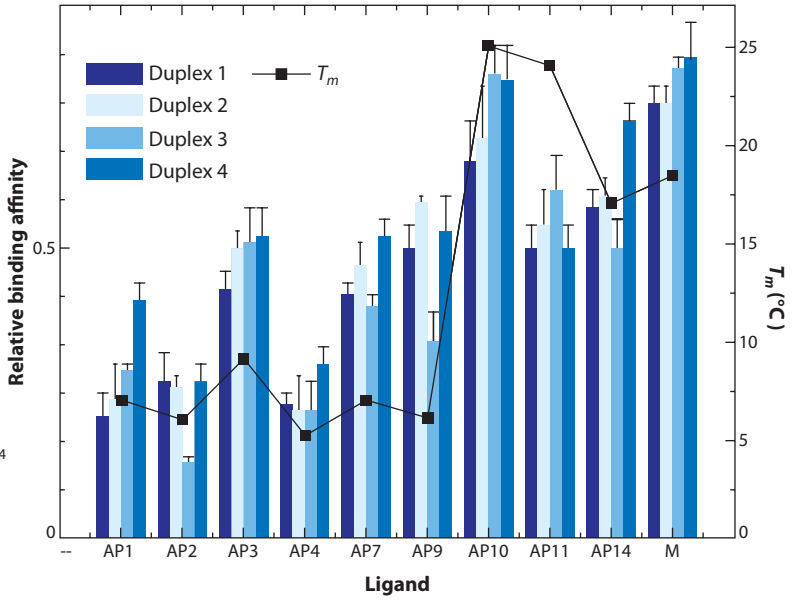

Figure 6

Structures of anthrapyrazoles (APs) and summary of relative binding affinities based on electrospray ionization mass spectrometry measurements of fraction-bound DNA (*bar graph*) and the change in melting temperature (ΔT_m) of duplex/AP complexes (*right axis*). Abbreviation: M, mitoxantrone. Reprinted with permission from Reference 27. Copyright 2007, Wiley Interscience.

and *trans*-**D1** were evaluated for a series of duplexes containing general DNA motifs identified by companion DNAse I footprinting experiments. Experiments involving *trans*-**D1** indicated that the ligand bound extensively to a duplex containing the target sequence 5′-CAGTGA-3′. In contrast, *cis*-**C1** exhibited the most specific binding to the 5′-GGTACC-3′ sequence.

The DNA-binding properties of a series of anthrapyrazoles (APs; **Figure 6**), a class of anticancer drugs evolved from anthracyclines but with lower cardiotoxicities, were examined by ESI-MS (27). The structures of APs, which contain a pyrazole ring fused to a tricyclic anthraquinone, encourage intercalation into DNA. Relative binding affinities estimated from the ESI-MS data on the basis of the fraction of bound DNA for DNA/AP mixtures are summarized in **Figure 6**. The fraction-bound values correlated with the shifts in melting points of the DNA duplexes, which are also shown in **Figure 6**. (Mitoxantrone, an anthracenedione anticancer agent, was also included for comparative purposes.) Among the APs studied, AP10 yielded the highest fraction of bound DNA, and therefore showed the greatest relative binding affinity. Replacement of a chlorine atom for the hydroxyl group at the terminus of the pyrazole side chains (i.e., AP3 and AP4) resulted in a notable decrease (25%) in the fraction of bound DNA. For the pair AP1/AP2, the substitution of the chlorine atom did not significantly change the fraction of bound DNA, nor did the replacement of a methyl group with a hydrogen atom on the amino side chain in the pair AP2/AP4. However, the exchange of a methyl group with a hydrogen atom increased the fraction of bound DNA for the pairs AP1/AP3 and AP11/AP10 by 20%. Compared with the other ligands, the notable structural features that were presumed to contribute to the high affinity of AP10 included the absence of a methyl group on its amino side chain, the incorporation of a hydroxyl group at the terminus of the side chain, and the presence of a second amine chain located on the same side of the AP as the first amine side chain.

The ESI-MS trends were compared with (*a*) the change in melting temperature (ΔT_m) of DNA caused by its interaction with the APs and (*b*) the outcomes of cell-growth inhibition (27). Because DNA is typically stabilized by interaction with intercalating compounds, the temperature at which the DNA undergoes denaturation generally increases with intercalation. The ΔT_m values ranged from 5.2°C to 25°C for calf thymus DNA in the presence of the APs, and these values are mapped in **Figure 6** for each AP. Binding of AP4 caused the smallest change in melting temperature, thus reflecting its weak interaction with DNA. This low ΔT_m value mirrors the low relative binding affinity (i.e., fraction-bound DNA) determined from the ESI-MS analysis. On average, AP1, AP2, and AP4 yielded the lowest fraction-bound values by ESI-MS (0.29, 0.23, and 0.24, respectively), and the ΔT_m values for these three APs ranged from 5.2°C to 7°C. The three AP ligands that caused the greatest shift in melting temperature included AP10, AP11, and AP14, all of which yielded the highest fraction-bound values by ESI-MS (0.73, 0.54, and 0.60, respectively).

Analysis of growth-inhibition human leukemia K562 cells that were exposed to varying concentrations of the APs was also undertaken (27). The results were reported as K562 IC_{50} values that signified the 50% cell growth–inhibitory concentration. The K562 IC_{50} values ranged from a low of 0.11 μM for AP10 (most potent) to a high of 11 μM for AP4 (least potent). AP10, which yielded the greatest relative binding affinity in the ESI-MS measurements, was the most potent based on the cell growth–inhibition assay (K562 $IC_{50} = 0.11$ μM). The six compounds with the lowest potency (AP1, AP2, AP3, AP4, AP7, and AP9 with K562 IC_{50} values ranging from 1.8 to 11 μM) displayed the lowest relative binding affinities. Overall, the DNA-binding affinities of the APs obtained by ESI-MS screening correlated with their inhibitory activities. ESI-MS has also been used to evaluate the complexation of other types of novel ligands (28–40), including acridines (31), cationic porphyrins (36), cryptolepine alkaloids (37), protoberbine alkaloids (38), benzopyridoindole and benzopyridoquinoxaline compounds (32), and acridine- and naphthalene-derived macrocyclic bis-intercalators (33), with DNA duplexes.

2.2. Electrospray Ionization Mass Spectrometry Analysis of Quadruplex DNA/Drug Complexes

In addition to the ability to transfer duplexes to the gas phase, ESI also allows quadruplexes to be analyzed by MS. G-quadruplex DNA comprises three or more consecutive tetrads assembled from the guanine bases of up to four DNA strands (**Figure 7**) (4). The central cavity of the guanine

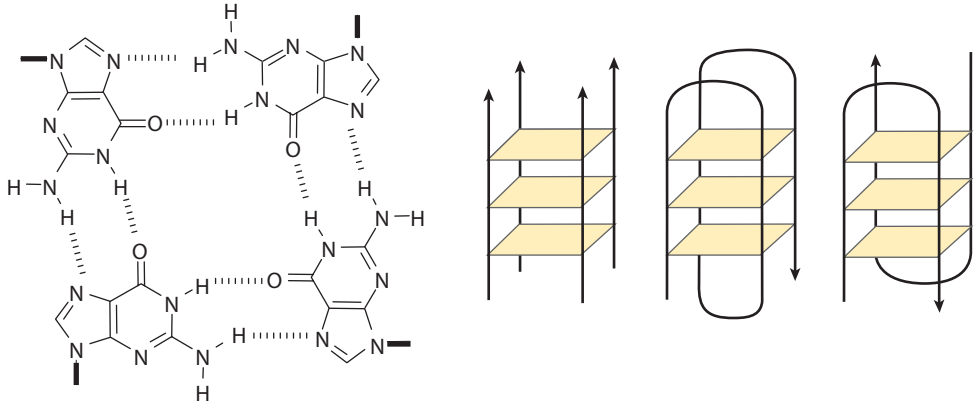

Figure 7

G-tetrad (*left*) and -quadruplex (*right*) structures.

tetrad affords a binding site for metal ions, which are essential for quadruplex formation. The three main types of quadruplexes include those composed of four parallel DNA strands; those composed of one DNA strand folded intramolecularly, and those consisting of two DNA strands in various orientations (see **Figure 7**). An ion-mobility and molecular-modeling study of a four-stranded complex, $[4(dTGGGT) + 3NH_4 - 8H]^{5-}$, indicated that the cross section of the ion matched most closely with a quadruplex structure, suggesting that the higher-order structure of the DNA was maintained upon transfer to the gas phase (41).

Just as ESI-MS can be used to evaluate duplex/ligand complexes, it can also be utilized to investigate the sequence selectivity and the relative binding affinities of quadruplex-interactive ligands. For example, the first study of quadruplex/ligand complexes by ESI-MS assessed the selectivity, binding stoichiometry, and mode of binding of Tel01 (shown in **Figure 8**), distamycin A, and diethylthiocarbocyanine iodide (42). The 1:2 quadruplex/ligand complexes identified by ESI-MS were consistent with the expected end-stacking binding mode. Comparisons of solutions containing quadruplexes versus duplexes with each ligand revealed that only Tel01 exhibited unique selectivity for quaduplex binding.

ESI-MS and companion spectroscopic studies were used to evaluate the association of a series of perylene diimide ligands (shown in **Figure 8**) with G-quadruplex DNA (43). Three of the ligands—PIPER, Tel11, and Tel18—exhibited substantial complexation with duplex DNA and/or

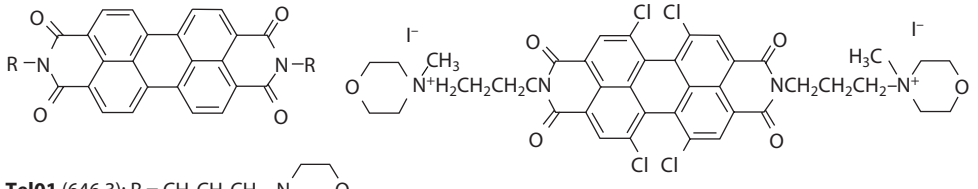

Tel01 (646.3): R = $CH_2CH_2CH_2$–N⟨O⟩

Tel18 (812.2)

PIPER (614.3): R = CH_2CH_2–N⟨⟩

Tel11 (676.6): R = $CH_2CH_2CH_2$–N^+(⟨O⟩, H_3C), I^-

Tel12 (632.1): R = $CH_2CH_2CH_2PO(OK)_2$

Ligand	Quadruplex	Duplex	Single strand
Tel01	0.65	0.20	--
PIPER	0.95	0.80	--
Tel11	0.95	0.95	0.10
Tel12	0.30	--	--
Tel18	0.75	0.90	0.10

Figure 8

Structures of perylene diimide ligands and binding selectivities based on fraction-bound values obtained by electrospray ionization mass spectrometry. Adapted with permission from Reference 43. Copyright 2006, Elsevier.

single-stranded DNA, confirming the ligands' lack of selectivity. However, two others—Tel01 and Tel12—demonstrated high selectivity for G-quadruplex DNA. Fluorescence quenching experiments of the perylene diimides in the presence of DNA gave further insight into the affinity and selectivity differences of these ligands for G-quadruplex DNA. In general, the fluorescence of DNA-interactive ligands is quenched upon binding to DNA. Tel01 exhibited great selectivity for G-quadruplex DNA binding, as shown by the minimal fluorescence quenching in the presence of either duplex or single-stranded DNA compared with G-quadruplex DNA. Other ligands, such as PIPER and Tel11, appeared to interact more strongly with G-quadruplex DNA when compared with Tel01, but they showed very little selectivity for G-quadruplex DNA versus duplex DNA. Both Tel11 and Tel18 also showed significant interactions with single-stranded DNA. Tel12 did not interact strongly with G-quadruplex DNA, as evidenced by the low magnitude of fluorescence quenching.

Solutions containing the G-quadruplex and one of each of the five nonbenzannulated ligands (Tel01, Tel11, Tel12, Tel18, and PIPER) exhibited 1:1 and 1:2 binding stoichiometries. ESI mass spectra of solutions containing the perylene diimide ligands with duplex DNA or single-stranded DNA were evaluated to assess selectivity for these different DNA structures (43). Some ligands, such as Tel18, formed numerous complexes with the duplex DNA. The relative binding affinities of the ligands were evaluated on the basis of measurements of fraction-bound values obtained by measuring the abundances of free DNA ions and DNA/ligand complexes in the ESI mass spectra. These results are summarized in **Figure 8**. Although PIPER, Tel11, and Tel18 formed complexes with the quadruplex DNA, these three ligands also bound to duplex DNA. Both Tel11 and Tel18 also bound to single-stranded DNA, suggesting that the cationic side chains of the ligands promoted indiscriminant binding to DNA due to electrostatic interactions with the anionic phosphate backbone.

The interactions of three platinum-based complexes—bipyridine ethylenediamine platinum(II) (Pt1), phenylphenanthroimidazole ethylenediamine platinum(II) (Pt2), and naphthylphenanthroimidazole ethylenediamine platinum(II) (Pt3) (see **Figure 9**)—with quadruplex DNA were evaluated by ESI-MS (44). These complexes were designed to incorporate extended aromatic pi surface areas to enhance their end-stacking interactions with quadruplex DNA. Companion circular dichroism experiments were undertaken to characterize the structure of the quadruplexes as well as to monitor changes in the melting points upon binding of the metal complexes. The percentages of bound DNA to the three platinum-based ligands are summarized in **Figure 9** on the basis of ESI-MS measurements of ion abundances. The highest quadruplex affinities were obtained for the two phenanthroimidazole platinum–based ligands (Pt2 and Pt3), which had a notable dependency on the type of quadruplex: The affinities for parallel intramolecular quadruplexes possessing shorter loop regions were much lower than for the antiparallel quadruplexes with elongated loops between guanine repeats. Binding to single-stranded and duplex DNA was minimal for the platinum complexes. Thermal denaturation studies (i.e., DNA melting-point experiments) demonstrated that the two platinum complexes, Pt2 and Pt3, significantly stabilized the quadruplexes relative to ruthenium complexes. The increase in melting point caused by binding of the platinum complexes ranged from 18°C to 22°C, compared with increases of 4°C or less for ruthenium complexes such as those containing bis(2,2′-bipyridine)(4,7-diphenyl-1,10-phenanthroline)ruthenium(II).

In the context of assessing quadruplex binding, ESI-MS has also been used to investigate other ligands (45–53). These include the antitumor drug ditercalinium (45), a series of ethidium analogs (46), the alkaloid cryptolepine (47), both perylene and coronene analogs (52), the planar photooxidizing trioxatriangulenium ion (53), a pyrrole-inosine nucleotide (51), and an indolyl berberine derivative (49).

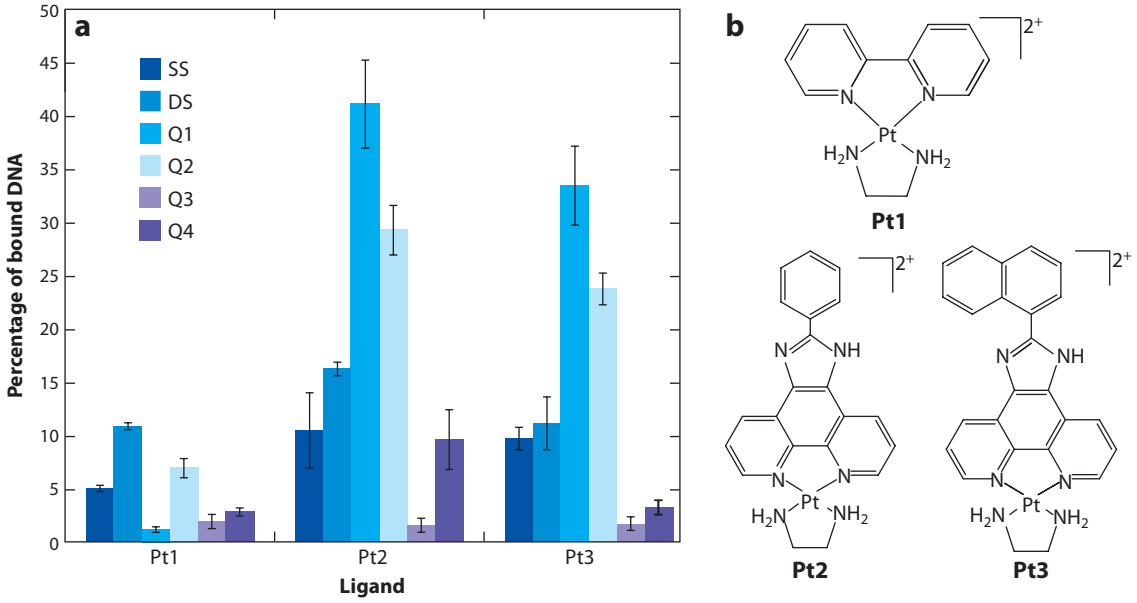

Figure 9

(*a*) Chart of ligand-binding ratios for three platinum ligands with quadruplex, duplex, and single-stranded sequences. Abbreviations: DS, d(GCGCGGAACCGCGC/dGCGCGGTTCCGCGC); Q1,[d($T_4G_4T_4$)]$_4$; Q2,d($T_4G_4T_4G_4T_4G_4T_4G_4T_4$); Q3, d($T_2G_4T_2G_4T_2G_4T_2G_4$); Q4, d($T_2AG_3T_2AG_3T_2AG_3T_2AG_3$); SS, d(GCGCGGAACCGCGC). (*b*) The structures of the platinum ligands. Abbreviations: Pt1, bipyridine ethylenediamine platinum(II); Pt2, phenylphenanthroimidazole ethylenediamine platinum(II); Pt3, naphthylphenanthroimidazole ethylenediamine platinum(II). Adapted from Reference 44. Copyright 2009, Wiley Periodicals.

3. TANDEM MASS SPECTROMETRY FOR CHARACTERIZATION OF DNA/LIGAND COMPLEXES

MS/MS has proven to be a versatile way to sequence biopolymers such as DNA (54). Thus, a natural extension of this technique has been the use of MS/MS to determine the putative binding modes of DNA/ligand complexes (18, 20, 55). DNA duplexes dissociate in the gas phase by one of two major routes: strand separation to yield two single-stranded species or covalent cleavage to yield either fragments of single strands (formation of *a–B* and *w* ions) or partial duplexes, from which either base loss or backbone fragmentation of one strand has occurred. The tendency for covalent cleavage increases with the number of interstrand hydrogen bonds, that is, for longer versus shorter duplexes and G/C-rich versus A/T-rich sequences. Typically, duplexes in higher charge states tend to favor strand separation upon activation, a process that stems from destabilization of the native duplexes by internal Coulombic repulsion due to the large number of charges. Duplexes in lower charge states preferentially undergo base loss and covalent cleavage to form *a–B* and *w* ions.

Complexes between DNA and intercalator ligands typically dissociate via the ejection of the ligand, producing the ligand-free duplex, or by separation of the single strands of the duplex, with the ligand remaining bound to one of the strands (55). For lower charge states, ejection of either a neutral or a deprotonated drug molecule also routinely occurs for DNA/intercalator complexes. Formation of *a–B* and *w* sequence ions, pathways observed upon dissociation of the free duplexes, is not observed.

For complexes containing minor groove binders in the lower charge states, base loss and covalent cleavage (i.e., formation of *a–B* and *w* ions) are generally favored over loss of the ligand,

and these complexes do not simply disassemble by strand separation (55). For complexes in the higher charge states, strand separation and base loss are dominant. In general, the fragmentation patterns for the lower-charge-state DNA/ligand complexes are thought to be more characteristic of specific drug/DNA interactions because Coulombic effects are less notable.

Infrared multiphoton dissociation (IRMPD) is an alternative to collision-activated dissociation for generation of characteristic fragmentation patterns of DNA ions (56). The large photoabsorptive cross section of the phosphate backbone at 10.6 μm promotes extremely efficient energization and dissociation within short irradiation times (<2 ms at 50 W). Upon IRMPD, strand-separation pathways are dominant for DNA/ligand complexes containing A/T-rich sequences and/or minor groove–binding drugs. In contrast, loss of the ligand is favorable for complexes containing intercalating drugs and/or duplexes with higher G/C-base content. Of particular significance is that the base-loss pathways that dominate collision-induced dissociation (CID) of DNA complexes are minimized upon IRMPD due to the secondary activation and dissociation of these base-loss ions that occur upon IRMPD. For duplex/ligand complexes in lower charge states, simple strand separation with or without retention of the ligand does not occur; instead, sequence ions (*a–B*, *w*) of the individual DNA strands are favored for the complexes. The ligand-loss pathway is predominant for complexes containing the intercalator ligands.

4. USE OF CHEMICAL PROBES TO CHARACTERIZE DNA/LIGAND COMPLEXES

The results and examples discussed above demonstrate the vast capabilities of ESI-MS for determining binding affinities and selectivities of DNA-interactive ligands and also provide general information about binding modes that can be obtained from MS/MS of the noncovalent DNA/ligand complexes. However, ESI-MS alone or even in conjunction with MS/MS strategies gives limited information about ligand-binding sites or concomitant changes in DNA structure. Combining ESI-MS with the use of chemical probes (57, 58) that react with and modify nucleic acids in a structure-dependent manner provides a more versatile approach to investigating ligand-binding sites and understanding how interactions of ligands with DNA can alter its conformation. Chemical probes in conjunction with ESI-MS have been used for both RNA and DNA substrates (44, 59–61). Investigation of the impact of ligand binding on DNA conformations was first reported for reactions of $KMnO_4$, an oxidizing agent that reacts primarily by attacking the double bond of thymine to produce a mixture of diol and an alpha-hydroxylketone product, which leads to product mass shifts of 34 and 32 Da, respectively (**Figure 10**) (61). In general, only thymines in unstacked, single-stranded DNA are oxidized by $KMnO_4$, whereas double-stranded DNA is resistant (62). Upon ligand intercalation, DNA frequently undergoes unwinding and elongation, thus making previously stacked thymines accessible to oxidative attack by $KMnO_4$.

Oxidation of single-stranded DNA by $KMnO_4$ was extensive; each thymine was accessible and reactive based on the ESI-MS spectra due to the abundances of the DNA ions and the new mass-shifted adducts that emerged after exposure of the DNA to $KMnO_4$ (61). Duplex DNA was far more resistant to oxidation because of the stacking of the nucleobases, which sterically hindered the access and attack of the permanganate ion on the double bond of thymine. The oxidation of the DNA/ligand complexes depended on whether the ligands bound in such a way that they blocked access to the thymines or increased access to the thymines due to distortion of the DNA. For example, intercalation generally increased the reactivity of thymines due to the favorable change in DNA conformation. Results that illustrate this phenomenon are shown in **Figure 11** for complexes consisting of a duplex and echinomycin, which is a bis-intercalator antibiotic that binds to duplex DNA [d(GCGGATATATGGCG/CGCCATATATCCGC)] via

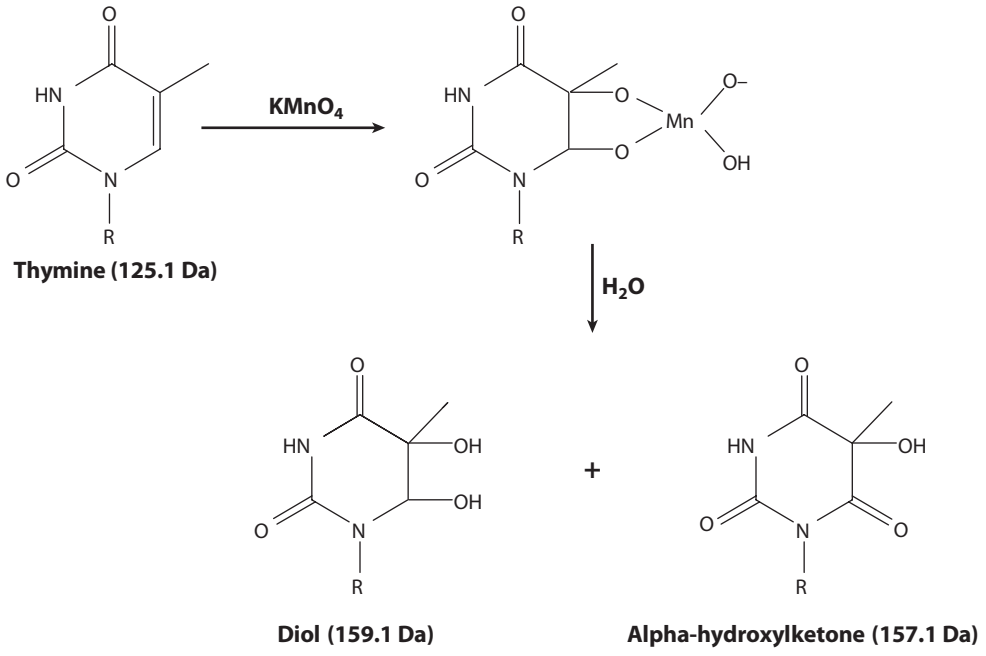

Figure 10

Mechanism of permanganate oxidation of thymine nucleobases. The mass of thymine and the resulting diol and alpha-hydroxylketone products are shown in parentheses. Reprinted with permission from Reference 61. Copyright 2007, American Chemical Society.

the intercalation of two quinoxaline chromophores at CpG sites, with the central bicyclic peptide residing in the minor groove (see structure in **Figure 1**). The ESI mass spectra obtained for a solution containing the duplex alone, the duplex with echinomycin, and the reaction of the duplex/echinomycin complexes with $KMnO_4$ are shown in **Figure 11**.

The degrees of oxidation of the DNA complexes shown in **Figure 11** were compared in a semiquantitative manner on the basis of calculations of percent oxidation values:

$$\text{Percent oxidation} \frac{A_{[M+O]} + 2A_{[M+2\times O]} + \ldots nA_{[M+n\times O]}}{A_{[M]} + A_{[M+O]} + 2A_{[M+2\times O]} + \ldots nA_{[M+n\times O]}} \times 100,$$

where $A_{[M]}$ is the ion abundance of the species designated in the subscript bracket, $A_{[M+O]}$ corresponds to each complex containing one or more oxidation adducts, and n is the maximum number of oxidation adducts associated with the particular DNA/ligand complex [M] (61). For the spectra shown in **Figure 11**, the percent oxidation of the free duplex is 15%, and the oxidation values of the corresponding DNA/echinomycin complexes are 68% for the 1:1 complex, 76% for the 1:2 complex, and 88% for the 1:3 complex (all in the 6− charge state). These results underscore the fact that the multiple intercalations of echinomycin caused a significant distortion of double-stranded DNA, which increased the accessibility of thymines to the oxidation reactions.

The length of the duplex length also influenced the $KMnO_4$ oxidation reaction (61). Experiments involving a seven–base pair duplex, d(GCAGTGA/TCACTGC), and a longer 21–base pair duplex, d(GGACAGTGAGGGCAGTGAGGG/CCCTCACTGCCCTCACTGTCC), showed that the percent oxidation value for the $[ds]^{3-}$ ion of the shorter sequence after $KMnO_4$ reaction in the absence of any DNA-interactive ligand was determined to be 66%, suggesting

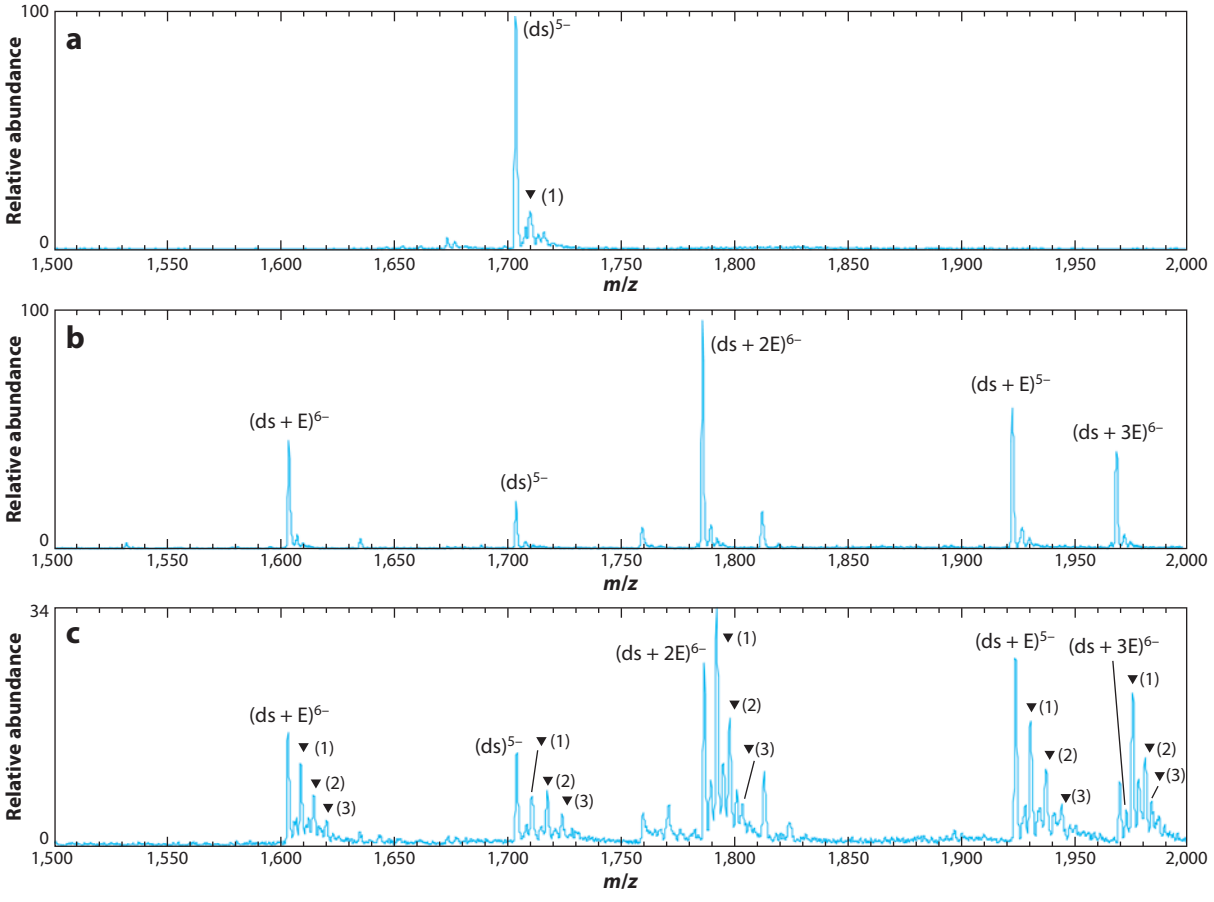

Figure 11

Electrospray ionization mass spectra showing solutions containing the duplex d(GCGGATATATGGCG/CGCCATATATCCGC) (ds) (*a*) 20 min after reaction with $KMnO_4$, (*b*) with echinomycin (E) prior to reaction with $KMnO_4$, and (*c*) with E 20 min after reaction with $KMnO_4$. Relative to the oxidation of the duplex alone, the degree of oxidation is much greater for the DNA/E complexes. The degree of oxidation also changed with the stoichiometry of the complex; as the number of bound ligands increased, the abundance of the oxidized ions increased relative to the unoxidized ions. The degree of oxidation is greatest for the 1:3 DNA/E complexes due to the unwinding and elongation of the duplex, which make thymines in the duplex more accessible for reaction with $KMnO_4$. Ions containing oxidized thymines are labeled with triangles; numbers in parentheses indicate the numbers of oxidation adducts. Reprinted with permission from Reference 61. Copyright 2007, American Chemical Society.

more extensive distortion of the shorter duplex. The percent oxidation was determined to be 39% for the longer duplex (61). After echinomycin binding, the percent oxidation value of the 1:1 echinomycin/duplex complexes was determined to be 60%, and the value for the 2:1 complexes was 74% for the longer duplex.

Oxidation reactions with complexes containing other types of DNA-interactive ligands, including three other intercalators and a minor groove binding agent, were also examined by ESI-MS (61). The mono-intercalator actinomycin D binds to DNA duplexes via the intercalation of the phenoxazone chromophore and the two cyclic peptides interacting with the minor groove. As a monointercalator, the unwinding angle and elongation of the duplex upon actinomycin D binding were less substantial compared with the bis-intercalator echinomycin. The percent oxidation value

for this duplex in the absence of ligand was determined to be 20%, and the percent oxidation for the 1:1 complexes was calculated to be 21%—not significantly different from the percent oxidation of the duplex in the absence of the ligand. Oxidation of a complex containing the threading bis-intercalator, *cis*-**C1** (see structure in **Figure 5**), resulted in an oxidation value of 42%. In the absence of the bis-intercalator ligand, the percent oxidation of the duplex was 20%. The duplex distortion induced by *cis*-**C1** was considerably greater than that caused by actinomycin with the same duplex (only 21%) because actinomycin is a monointercalator, whereas *cis*-**C1** is a bis-intercalator. The sites of oxidation of the DNA/ligand complexes were determined by use of CID to create fragmentation patterns in which certain sequence ions retained the oxidation adduct, as reflected by mass shifts in those ions. Upon CID, the mass spectra of the oxidized DNA/ligand complexes displayed diagnostic *a–B* and *w* sequence ions, only some of which contained the mass shift characteristic of the oxidized base. On the basis of the cleavage pattern and correlation of the mass-shifted fragment ions, the locations of the oxidized residues could be identified.

Another chemical probe strategy that proved to be useful for the investigation of conformation changes of DNA upon ligand binding entails the use of glyoxal (44). In this approach, solutions containing various DNA structures (i.e., an intermolecular four-stranded quadruplex, its constituent single strand, or complexes composed of a quadruplex with a platinum compound) were incubated with glyoxal, a reagent that selectively reacts with accessible guanines. The extent of reaction of glyoxal with the DNA was calculated by dividing the summed abundances of all the glyoxal-adducted DNA ions by the summed abundances of all the DNA species (both unreacted DNA and the DNA/glyoxal adducts). The individual single-stranded DNA exhibited substantial reactivity with glyoxal, as expected for flexible DNA structures in which the guanines should be accessible. The reactivity of the quadruplex with glyoxal decreased by a factor of four relative to that of the single strand, presumably because the Hoogsteen hydrogen bonds between the guanine bases of the quadruplex Q1 blocked access to and/or suppressed the reactions of glyoxal. Interaction of Q1 with Pt1 caused negligible change in the reactivity of the quadruplex. (The structures of the platinum complexes are shown in **Figure 9**). However, interaction of Q1 with Pt2 increased the extent of reaction of the quadruplex with glyoxal by a factor of two, indicating that Pt2 increases the accessibility of some of the guanine bases by altering the structure of the quadruplex.

This type of ESI-MS methodology offers an attractive alternative to traditional gel-based chemical probe experiments, as it eliminates the need to use both radiolabeled DNA and the piperidine heat treatment often required to identify the sites of reaction upon cleavage of the DNA. Moreover, the use of chemical probes in conjunction with ESI-MS analysis offers excellent sensitivity and facile adaptation to high-throughput screening applications.

5. CONCLUSIONS

ESI-MS is now considered a versatile method for investigating DNA/ligand complexes, particularly in the context of affirming the stoichiometries of complexes and estimating both DNA-binding affinities and sequence selectivities for series of ligands. The minimal sample consumption and high sensitivity afforded by ESI-MS make it a natural choice for screening studies involving new ligands, especially compared with nuclear magnetic resonance methods, which typically require far more sample. Additional information about the modes and sites of ligand interactions can be obtained by characterizing the complexes by MS/MS or in conjunction with the use of chemical probes that reveal changes in DNA conformations and accessibility of nucleobases upon ligand binding. ESI-MS can be adapted to high-throughput screening applications to identify promising DNA-interactive ligands. Such ligands can be subsequently studied in greater detail by

conventional methods, such as nuclear magnetic resonance and spectrophotometric techniques, which can provide more extensive structural and/or quantitative binding constant information. Because the ESI-MS methods for evaluating noncovalent complexes are becoming more established, the ability to investigate even more elaborate macromolecular complexes, such as those containing DNA, ligands, and relevant proteins, is ushering in a provocative new area of exploration.

DISCLOSURE STATEMENT

The author is not aware of any affiliations, memberships, funding, or financial holdings that might be perceived as affecting the objectivity of this review.

ACKNOWLEDGMENTS

This work was supported by the Robert A. Welch Foundation (F-1155) and the National Institutes of Health (RO1 GM65956).

LITERATURE CITED

1. Goodman LS, Hardman JG, Limbird LE, Gilman AG, eds. 2001. *Goodman and Gilman's The Pharmacological Basis of Therapeutics*. New York: McGraw-Hill. 10th ed.
2. Braña MF, Cacho M, Gradillas A, de Pascual-Teresa B, Ramos A. 2001. Intercalators as anticancer drugs. *Curr. Pharm. Des.* 7:1745–80
3. Bischoff G, Hoffmann S. 2002. DNA-binding drugs used in medicinal therapy. *Curr. Med. Chem.* 9:321–48
4. Kerwin SM. 2000. G-quadruplex DNA as a target for drug design. *Curr. Pharm. Des.* 6:441–71
5. Boer DR, Canals A, Coll M. 2009. DNA-binding drugs caught in action: the latest 3D pictures of drug-DNA complexes. *Dalton Trans.* 3:399–414
6. Eckhardt S. 2002. Recent progress in the development of anticancer agents. *Curr. Med. Chem. Anti-Cancer Agents* 2:419–39
7. Rosu F, De Pauw E, Gabelica V. 2008. Electrospray mass spectrometry to study drug–nucleic acid interactions. *Biochimie* 90:1074–87
8. Hofstadler SA, Griffey RH. 2001. Analysis of noncovalent complexes of DNA and RNA by mass spectrometry. *Chem. Rev.* 101:377–90
9. Beck JL, Colgrave ML, Ralph SF, Sheil MM. 2001. Electrospray ionization mass spectrometry of oligonucleotide complexes with drugs, metals, and proteins. *Mass. Spectrom. Rev.* 20:61–87
10. Fenn JB, Mann M, Meng CK, Wong SF, Whitehouse CM. 1989. Electrospray ionization for mass spectrometry of large biomolecules. *Science* 246:64–71
11. Light-Wahl KJ, Spring DL, Winger BE, Edmonds CG, Camp DG, et al. 1993. Observation of a small oligonucleotide duplex by electrospray ionization mass spectrometry. *J. Am. Chem. Soc.* 115:803–4
12. Gale DC, Smith RD. 1995. Characterization of noncovalent complexes formed between minor groove binding molecules and duplex DNA by electrospray ionization–mass spectrometry. *J. Am. Soc. Mass Spectrom.* 6:1154–64
13. Gale DC, Goodlett DR, Light-Wahl KJ, Smith RD. 1994. Observation of duplex DNA-drug noncovalent complexes by electrospray ionization mass spectrometry. *J. Am. Chem. Soc.* 116:6027–28
14. Kapur A, Beck JL, Sheil MM. 1999. Observation of daunomycin and nogalamycin complexes with duplex DNA using electrospray ionization mass spectrometry. *Rapid Commun. Mass Spectrom.* 13:2489–97
15. Colgrave ML, Beck JL, Sheil MM, Searle MS. 2002. Electrospray ionization mass spectrometric detection of weak non-covalent interactions in nogalamycin-DNA complexes. *Chem. Commun.* 2002:556–57
16. Gabelica V, De Pauw E, Rosu F. 1999. Interaction between antitumor drugs and a double-stranded oligonucleotide studied by electrospray ionization mass spectrometry. *J. Mass Spectrom.* 34:1328–37
17. Wan KX, Shibue T, Gross ML. 2000. Non-covalent complexes between DNA-binding drugs and double-stranded oligodeoxynucleotides: a study by ESI ion-trap mass spectrometry. *J. Am. Chem. Soc.* 122:300–7

18. Gabelica V, Rosu F, Houssier C, De Pauw E. 2000. Gas phase thermal denaturation of an oligonucleotide duplex and its complexes with minor groove binders. *Rapid Commun. Mass Spectrom.* 14:464–67
19. Greig MJ, Robinson JM. 2000. Detection of oligonucleotide-ligand complexes by ESI-MS (DOLCE-MS) as a component of high throughput screening. *J. Biomol. Screen.* 5:441–54
20. Wan KX, Gross ML, Shibue T. 2000. Gas-phase stability of double-stranded oligodeoxynucleotides and their noncovalent complexes with DNA-binding drugs as revealed by collisional activation in an ion trap. *J. Am. Soc. Mass Spectrom.* 11:450–57
21. Rosu F, Gabelica V, Houssier C, De Pauw E. 2002. Determination of affinity, stoichiometry and sequence selectivity of minor groove binder complexes with double-stranded oligodeoxynucleotides by electrospray ionization mass spectrometry. *Nucleic Acids Res.* 30:e82
22. Gabelica V, Galic N, Rosu F, Houssier C, De Pauw E. 2003. Influence of response factors on determining equilibrium association constants of non-covalent complexes by electrospray ionization mass spectrometry. *J. Mass Spectrom.* 38:491–501
23. Reyzer ML, Brodbelt JS, Kerwin SM, Kumar D. 2001. Evaluation of complexation of metal-mediated DNA-binding drugs to oligonucleotides via electrospray ionization mass spectrometry. *Nucleic Acids Res.* 29:e103
24. Oehlers L, Mazzitelli CL, Brodbelt JS, Rodriguez M, Kerwin S. 2004. Evaluation of complexes of DNA duplexes and novel benzoxazoles or benzimidazoles by electrospray ionization mass spectrometry. *J. Am. Soc. Mass Spectrom.* 15:1593–603
25. Mazzitelli CL, Rodriguez M, Kerwin SM, Brodbelt JS. 2008. Evaluation of metal-mediated DNA binding of benzoxazole ligands by electrospray ionization mass spectrometry. *J. Am. Soc. Mass Spectrom.* 19:209–18
26. Mazzitelli CL, Chu Y, Reczek JJ, Iverson BL, Brodbelt JS. 2007. Screening of threading bis-intercalators binding to duplex DNA by electrospray ionization tandem mass spectrometry. *J. Am. Soc. Mass Spectrom.* 18:311–21
27. Smith SI, Guziec LJ, Guziec FS, Hasinoff BB, Brodbelt JS. 2007. Evaluation of relative DNA binding affinities of anthrapyrazoles by electrospray ionization mass spectrometry. *J. Mass Spectrom.* 42:681–88
28. Gupta R, Kapur A, Beck JL, Sheil MM. 2001. Positive ion electrospray ionization mass spectrometry of double-stranded DNA/drug complexes. *Rapid Commun. Mass Spectrom.* 15:2472–80
29. Gupta R, Beck JL, Ralph SF, Sheil MM, Aldrich-Wright JR. 2004. Comparison of the binding stoichiometries of positively charged DNA-binding drugs using positive and negative ion electrospray ionization mass spectrometry. *J. Am. Soc. Mass Spectrom.* 15:1382–91
30. Chen WH, Quin Y, Cai Z, Chan CL, Luo GA, Jiang ZH. 2005. Spectrometric studies of cytotoxic protoberberine alkaloids binding to double-stranded DNA. *Bioorg. Med. Chem.* 13:1859–66
31. Smith SI, Guziec FS Jr, Guziec L, Brodbelt JS. 2009. Interactions of sulfur-containing acridine ligands with DNA by ESI-MS. *Analyst* 134:2058–66
32. Rosu F, Nguyen C, De Pauw E, Gabelica V. 2007. Ligand binding mode to duplex and triplex DNA assessed by combining electrospray tandem mass spectrometry and molecular modeling. *J. Am. Soc. Mass Spectrom.* 18:1052–62
33. Bahr M, Gabelica V, Granzhan A, Teulade-Fichou MP, Weinhold E. 2008. Selective recognition of pyrimidine-pyrimidine DNA mismatches by distance-constrained macrocyclic bis-intercalators. *Nucleic Acids Res.* 36:5000–12
34. Beck JL, Gupta R, Urathamakul T, Williamson NL, Sheil MM, et al. 2003. Probing DNA selectivity of ruthenium metallointercalators using ESI mass spectrometry. *Chem. Commun.* 2003:626–27
35. Urathamakul T, Beck JL, Sheil MM, Aldrich-Wright JR, Ralph SF. 2004. Comparison of mass spectrometry and other techniques for probing interactions between metal complexes and DNA. *Dalton Trans.* 17:2683–90
36. Ramos CIV, Barros CM, Fernandes AM, Santana-Marques MG, Ferrer Correia AJ, et al. 2005. Interactions of cationic porphyrins with double-stranded oligodeoxynucleotides: a study by electrospray ionisation mass spectrometry. *J. Mass Spectrom.* 40:1439–47
37. Guitta L, Alberti P, Rosu F, Miert SV, Thetiot E, et al. 2003. Interactions of crytolepine and neocryptolpetine with unusual DNA structures. *Biochimie* 85:535–47

38. Chen WH, Chan CL, Cai Z, Luo GA, Jiang ZH. 2004. Study on noncovalent complexes of cytotoxic protoberbine alkaloids with double-stranded DNA by using electrospray ionization mass spectrometry. *Bioorg. Med. Lett.* 14:4955–59
39. Wang Z, Guo X, Liu Z, Cui M, Song F, Liu S. 2008. Studies on alkaloids binding to GC-rich human survivin promoter DNA using positive and negative ion electrospray ionization mass spectrometry. *J. Mass Spectrom.* 43:327–35
40. Rosu F, Pirotte S, De Pauw E, Gabelica V. 2006. Positive and negative ion mode ESI-MS and MS/MS for studying drug-DNA complexes. *Int. J. Mass Spectrom.* 253:156–71
41. Gidden J, Shammel Baker E, Ferzoco A, Bowers MT. 2005. Structural motifs of DNA complexes in the gas phase. *Int. J. Mass Spectrom.* 240:183–93
42. David WM, Brodbelt J, Kerwin SM, Thomas PW. 2002. Investigation of quadruplex oligonucleotide-drug interactions by electrospray ionization mass spectrometry. *Anal. Chem.* 74:2029–33
43. Mazzitelli CL, Brodbelt JS, Kern JT, Rodriguez M, Kerwin SM. 2006. Evaluation of binding of perylene diimide and benzannulated perylene diimide ligands to DNA by electrospray ionization mass spectrometry. *J. Am. Soc. Mass Spectrom.* 17:593–604
44. Pierce SE, Kieltyka R, Sleiman HF, Brodbelt JS. 2009. Evaluation of binding selectivities and affinities of platinum-based quadruplex interactive complexes by electrospray ionization mass spectrometry. *Biopolymers* 91:233–43
45. Carrasco C, Rosu F, Gabelica F, Houssier C, De Pauw E, et al. 2002. Tight binding of the antitumor drug ditercalinium to quadruplex DNA. *ChemBioChem* 3:1235–41
46. Rosu F, De Pauw E, Guittat L, Alberti P, Lacroix L, et al. 2003. Selective interaction of ethidium derivatives with quadruplexes: an equilibrium dialysis and electrospray ionization mass spectrometry analysis. *Biochemistry* 42:10361–71
47. Guittat L, Alberti P, Rosu F, Van Miert S, Thetiot E, et al. 2003. Interactions of cryptolepine and neocryptolepine with unusual DNA structures. *Biochimie* 85:535–47
48. Gabelica V, Baker ES, Teulade-Fichou MP, De Pauw E, Bowers MT. 2007. Stabilization and structure of telomeric and c-myc region intramolecular G-quadruplexes: the role of central cations and small planar ligands. *J. Am. Chem. Soc.* 129:895–904
49. Gornall KC, Samosorn S, Talib J, Bremner JB, Beck JL. 2007. Selectivity of an indolyl berberine derivative for tetrameric G-quadruplex DNA. *Rapid Commun. Mass Spectrom.* 21:1759–66
50. Mazzitelli CL, Wang J, Smith JI, Brodbelt JS. 2007. Gas-phase stability of G-quadruplex DNA determined by electrospray ionization tandem mass spectrometry and molecular dynamics simulations. *J. Am. Soc. Mass Spectrom.* 18:1760–73
51. Pierce SE, Sherman CL, Jayawickramarajah J, Lawrence CM, Sessler JL, Brodbelt JS. 2008. ESI-MS characterization of a novel pyrrole-inosine nucleoside that interacts with guanine bases. *Anal. Chim. Acta* 627:129–35
52. Casagrande V, Alvino A, Bianco A, Ortaggi G, Franceschin M. 2009. Study of binding affinity and selectivity of perylene and coronene derivatives towards duplex and quadruplex DNA by ESI-MS. *J. Mass Spectrom.* 44:530–40
53. Pothukuchy A, Mazzitelli C, Salazar M, Brodbelt JS, Kerwin SM. 2005. Duplex and quadruplex DNA binding and photocleavage by trioxatriangulenium ion. *Biochemistry* 44:2163–72
54. Banoub JH, Newton RP, Esmans E, Ewing DF, Mackenzie G. 2005. Recent developments in mass spectrometry for the characterization of nucleosides, nucleotides, oligonucleotides and nucleic acids. *Chem. Rev.* 105:1869–915
55. Keller KM, Zhang J, Oehlers L, Brodbelt JS. 2005. Influence of initial charge state on fragmentation patterns for noncovalent drug/DNA complexes. *J. Mass Spectrom.* 40:1361–71
56. Wilson J, Brodbelt JS. 2007. Infrared multiphoton dissociation of duplex DNA/drug complexes in a quadrupole ion trap. *Anal. Chem.* 79:2067–77
57. Bui CT, Rees K, Cotton RGH. 2004. Current chemicals used for probing DNA conformational changes and detection of unknown mutations. *Curr. Pharmacogenomics* 2:325–32
58. Millard JT. 1999. Molecular probes of DNA structure. *Comp. Nat. Prod. Chem.* 7:81–103

59. Yu E, Fabris D. 2004. Toward multiplexing the application of solvent accessibility probes for the investigation of RNA three-dimensional structures by electrospray ionization–Fourier transform mass spectrometry. *Anal. Biochem.* 334:356–66
60. Yu E, Fabris D. 2003. Direct probing of RNA structures and RNA-protein interactions in the HIV-1 packaging signal by chemical modification and electrospray ionization Fourier transform mass spectrometry. *J. Mol. Biol.* 330:211–23
61. Mazzitelli CL, Brodbelt JS. 2007. Probing ligand binding to duplex DNA using $KMnO_4$ reactions and electrospray ionization tandem mass spectrometry. *Anal. Chem.* 79:4636–47
62. Bui CT, Rees K, Cotton RGH. 2003. Permanganate oxidation reactions of DNA: perspective in biological studies. *Nucleosides Nucleotides Nucleic Acids* 22:1835–55

Annual Review of
Analytical Chemistry

Volume 3, 2010

Contents

Indexes

Errata

An online log of corrections to *Annual Review of Analytical Chemistry* articles may be found at http://arjournals.annualreviews.org/errata/anchem.